Carpathian Journal of Earth and Environmental Sciences, August 2020, Vol. 15, No. 2, p. 327 – 337; Doi:10.26471/cjees/2020/015/133

EVALUATION OF URBAN AREAS BY REMOTE SENSING METHODS IN RELATION TO CLIMATIC CONDITIONS: CASE STUDY CITY OF TIMISOARA

Mihai Valentin HERBEI[1] & Florin SALA[2*]

Banat University of Agricultural Sciences and Veterinary Medicine "King Michael I of Romania" from Timisoara, Timișoara, 300645, Romania; [1]Remote Sensing and GIS, [2]Soil Science and Plant Nutrition
E-mail: florin_sala@usab-tm.ro

Abstract; The study used methods based on remote sensing to evaluate the urban area of Timisoara City in relation to the climatic conditions. Satellite images were taken from the Landsat 8 system. The study interval was between August 9, 2013 and August 7, 2018. The images were taken in August, an expressive month in thermal aspect for the studied area. The spectral information from the satellite images was analyzed using specific indices, such as: Land Surface Temp - LST, Normalized Difference Built-Up Index – NDBI, and Normalized Difference Vegetation Index – NDVI, respectively. For the interpretation of the values of the indices, the climatic data were taken into account for the period January - July of each analyzed year (P1 - P7, precipitation in January-July; T1-T7, average monthly temperature in January-July). There were registered very strong, negative and positive correlations (NDVI with NDBI, r = -0.998; LST with P7, r =-0.976; LST with T4, r =-0.984; NDVI with P7, r =0.900). Also, strong negative or positive correlations were recorded (LST with P6, r=-0.891; LST with T5, r =-0.889; NDVI with LST, r=0.824; NDVI with T4, r =0.883). Depending on the time factor (T), the variation of indices was described by smoothing spline model (LST vs. T), or by models of the type of polynomial equations of degree 2 (NDBI vs T, R^2 =0.965, $p < 0.05$; NDVI vs. T, R^2 =0.986, $p < 0.01$). Multiple regression analysis led to obtaining 3D and isoquant variation models of NDVI and LST indices depending on T7 and P6.

Key words: isoquant, LST, mathematical model, NDVI, NDBI, urban ecosystem

1. INTRODUCTION

Urban areas are ecosystems of high structural and functional complexity (Pickett et al., 2016). These areas include natural elements, sometimes strongly anthropic (parks, gardens, isolated trees, green spaces, etc.), access roads of different sizes (alleys, sidewalks, road lanes), parking, and of course buildings and constructions with different destinations as housing, recreational, agreement, commercial, industrial, and of course, people with their various activities are also considered (Anand et al., 2010; Heymans et al., 2019).

The urban space is analyzed from the perspective of landscape planning and change, urban development and perspectives, and different studies have communicated results in these directions of approach (Oncia et al., 2013a,b; Rakhshandehroo et al., 2016; Heymans et al., 2019).

Imaging analysis and techniques based on remote sensing are very useful and precise tools for studying and evaluating urban areas (Bianchin & Bravin, 2008; Du et al., 2014).

The Geospatial approach has been used in the study of urban areas from different perspectives, such as structural and functional, quality of life assessment (Merschdorf et al., 2020) and aspects of urban pollution (eg with NO_2 and SO_2) (Qin et al., 2017; Yuchechen et al., 2017).

Studies have been carried out to optimize the resolution of images for urban form detection (Tran et al., 2011), and methods, techniques and models of monitoring of urban areas based on remote sensing have been proposed and developed (Deng et al., 2019; Lahoti et al., 2019).

Some studies had as topics: buildings analysis (Tarantino & Figorito, 2011), planning, development and management or urban area (Nielsen, 2015;

Kadhim et al., 2016).

Different indices have been proposed and used for the analysis and characterization of urban areas, such as: Land Surface Temp - LST (Weng et al., 2004, 2018), Normalized Difference Vegetation Index - NDVI (Rouse et al., 1974), Normalized Difference Built-Up Index - NDBI (Zha et al., 2003). Indices of stress and thermal discomfort specific to urban areas, Surface Urban Heat Island - SUHI, Urban Heat Island - UHI, Urban Cool Island - UCI, Thermal Discomfort - DI etc. were also proposed and used (Rasul et al., 2015; Ishola et al., 2016; Zhou et al., 2018; Aram et al., 2019).

Also, images were used in different satellite systems for the analysis and characterization of urban areas (Wan et al., 2015; Kumar et al., 2017; Guha et al., 2018).

Thermal stress (TS), hot spots (HS), surface urban heat island (SUHI), urban heat island (UHI), thermal discomfort (DI index), are intensively studied issues, and of major interest for urban areas and quality of life (Liu & Zhang, 2011; Lehoczky et al., 2017; Zhou et al., 2018; Orusa & Mondino, 2019). In this context, there were approaches regarding the interdependence relationship between land use and surfaces temperature in urban areas (Rinner & Hussain, 2011).

Green space mapping (Chen et al., 2018; Deng et al., 2019), green space in relation to urban sustainable development evaluation (Van et al., 2017), urban development plan, vegetation monitoring (eg urban tree and classification trees (Matikainen & Karila, 2011; Moskal et al., 2011), have also been topics of current research in this direction.

The green areas in the urban environment have been studied in relation to various ecological, aesthetic, structural, functional criteria, and aspects of the urban ecosystem as a whole, as well as in relation to the conservation of the vegetation, the socio-demographic opinion of the population, etc. (Zobec et al., 2020).

The present study started from the hypothesis that Landsat 8 satellite images can provide spectral information for the analysis and characterization of the urban area studied in relation to the variation of climatic conditions.

2. MATERIALS AND METHODS

The study used specific indices (LST, NDBI, NDVI) calculated based on spectral bands from Landsat 8 satellite images, in order to analyze and characterize the Timisoara urban ecosystem (associated with thermal conditions, vegetation, and buildings), in relation to climatic conditions over a period for 5 years.

The Landsat 8 satellite system was used to obtain satellite images and spectral information (Planet Team, 2018), figure 1.

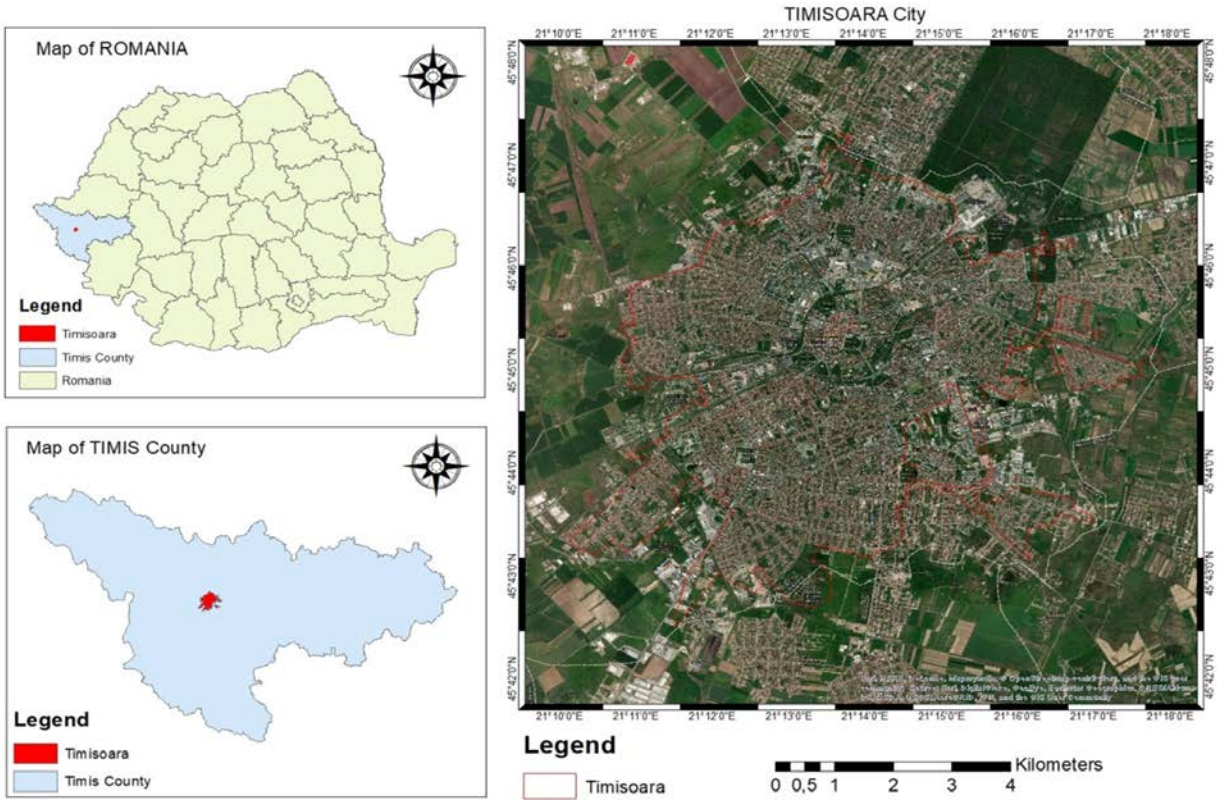

Figure 1. Timisoara City – general map

Images were taken in August, depending on the availability of images, as follows: August 9, 2013, August 15, 2015, August 4, 2017, and August 7, 2018, respectively. The study was conducted over a five-year time period (T).

Based on spectral bands and specific calculation formulas Land Surface Temp - LST (Weng et al., 2004), equation (1), Normalized Difference Built-Up Index - NDBI (Zha et al., 2003), equation (2), and Normalized Difference Vegetation Index - NDVI (Rouse et al., 1974), equation (3) were determined.

$$LST = T / [1 + (w \cdot T / p) \ln \varepsilon] \quad (1)$$

where:
LST – Land Surface Temperature (°K),
T- Apparent Brightness Temperature, T_{10} or T_{11} (°K),
w - wavelength of emitted radiance [mm],

$$p = h \cdot c / s \left(1.438 \cdot 10^{-2}\ mK\right) \quad (1a)$$

h -Planck's constant ($6.626 \cdot 10^{-34}$ Js)
s - Boltzmann constant ($1.38 \cdot 10^{-23}$ J/K)
c - velocity of light ($2.998 \cdot 10^{8}$ m/s)
ε - Land Surface Emissivity (LSE)

$$NDBI = (NIR - SWIR)/(NIR + SWIR) \quad (2)$$

$$NDVI = (NIR - R)/(NIR + R) \quad (3)$$

Climatic data, average monthly temperatures (ºC) and precipitation (mm) were taken into consideration in the months of January - July of each year in which satellite images were taken (SMT, 2013-2018).

The experimental data were analyzed by ANOVA test, correlation analysis, and regression analysis. Statistical safety parameters used in the results interpreting, were represented by the correlation coefficient (r), the regression coefficient (R^2), the average error ($\bar{\varepsilon}$), the parameter p, and F test. For the processing of satellite images and the calculation of LST, NDBI, NDVI indices, the software ArcGIS and ArcGIS Imagery (Esri, 2014) were used. PAST software (Hammer et al., 2001) and Wolfram Alpha (2020) software were used to analyze and process the experimental data.

3. RESULTS

The satellite images, Landsat 8 satellite system, captured in the spectral information the urban elements given by buildings and vegetation, expressed in terms of NDBI and NDVI indices. Associated with them was also recorded the variation of the LST index values, as expression of the proportions between buildings and vegetation. Data are presented in table 1, and the graphical distribution, in the form of maps, of the LST, NDBI and NDVI indices are presented in Figures 2-4.

The ANOVA test (for Alpha = 0.001) confirmed the safety of the experimental data and the presence of the variance in the data set ($F=9.0828$, $F_{crit}=3.1268$, $p<<0.001$).

The correlation analysis revealed various interdependencies, both between the determined indices (LST, NDBI, NDVI), as well as between indices and temperature, respectively precipitation. A very strong negative correlation was identified between NDVI and NDBI (r = -0.998), a strong positive correlation was found between LST and NDBI (r = 0.824), and the average negative correlation was found between LST and NDVI (r = -0.786).

Regarding the LST index, very strong correlations were found with P7 (r = -0.976) and T4 (r = -0.984), strong correlations with P6 (r = -0.891), with T1 (r = -0.821), and with T5 (r = -0.889), and moderate correlations with P2 (r = -0.789) and T3 (r = 0.762) respectively. NDVI had a very strong positive correlation with P7 (r = 0.900), strong correlation with T4 (r = 0.883), and moderate correlations with P6 (r = 0.752) and T5 (r = 0.794). Other correlations of lower intensity were also identified.

The level of correlation of LST and NDVI indices with precipitation amount (PAMT) was analyzed during January - July, respectively with temperatures average (TAVG) for the same period for each year studied.

Table 1. Data of LST, NDVI and NDBI indices and climatic conditions for City of Timisoara, 2013 - 2018

Year	Indices			Precipitation (P, mm)							Temperatures (T, ºC)						
	LST	NDBI	NDVI	P1	P2	P3	P4	P5	P6	P7	T1	T2	T3	T4	T5	T6	T7
2013	33.15686	-0.05473	0.242145	54.3	37	104.2	34.1	97.3	47.5	24.9	-1.5	0.6	5.7	11.3	16.3	19.4	21.5
2015	32.0458	-0.0335	0.214432	51.4	37.4	33.3	28.1	46.9	61.8	25	2.1	2.9	7.1	11.6	17.7	21.2	24.9
2017	33.94456	-0.05782	0.250366	8.7	19.4	26	55.9	53.8	58.8	19.4	-4.7	3.3	9.4	10.8	17.6	22.5	24.2
2018	27.98844	-0.11605	0.314672	58.4	44.8	67.3	28.1	51.6	80.3	72.5	3	2	4.6	16.4	20	21.3	22.6

P -precipitation (mm); T -emperatures (ºC); 1 -January, 2 -February, 3 -March, 4 -April, 5 -May, 6 -June, 7 -July.

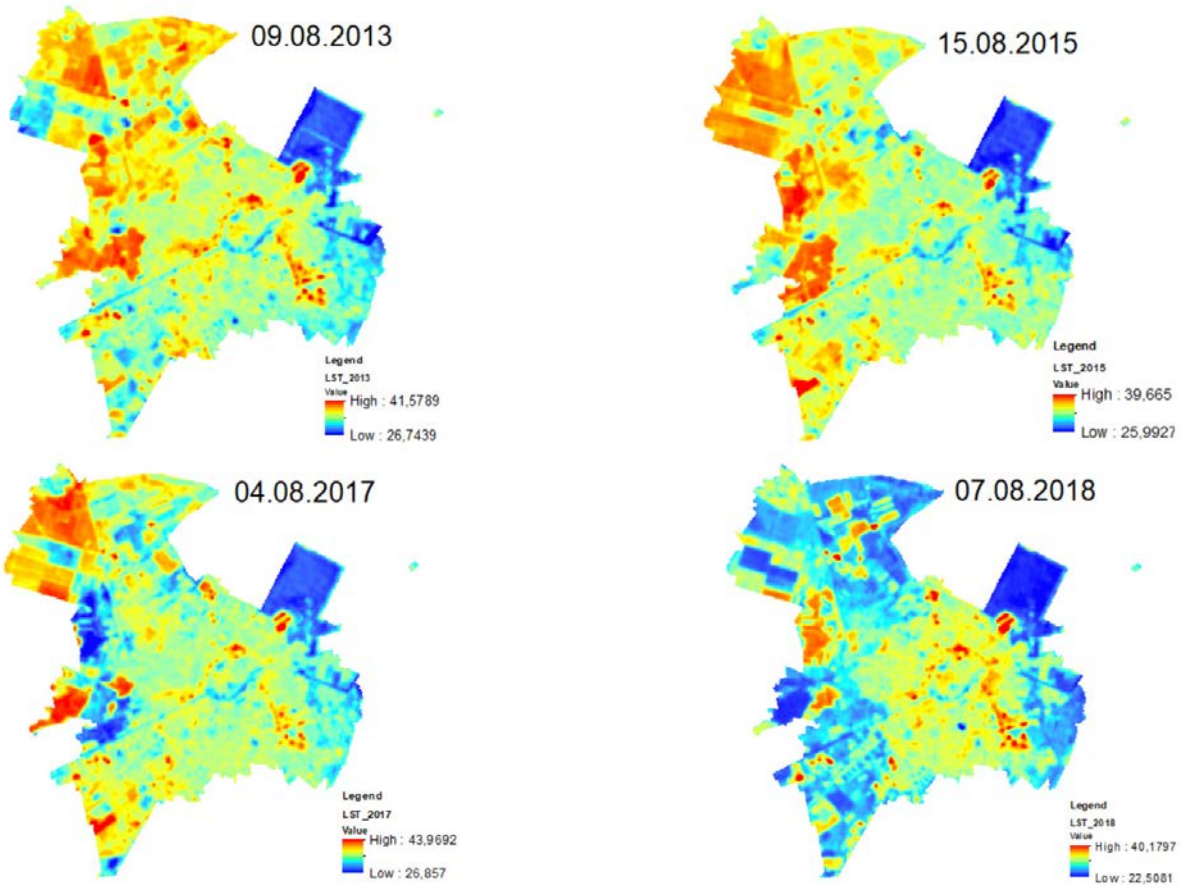

Figure 2. LST maps for Timisoara (2013 – 2018)

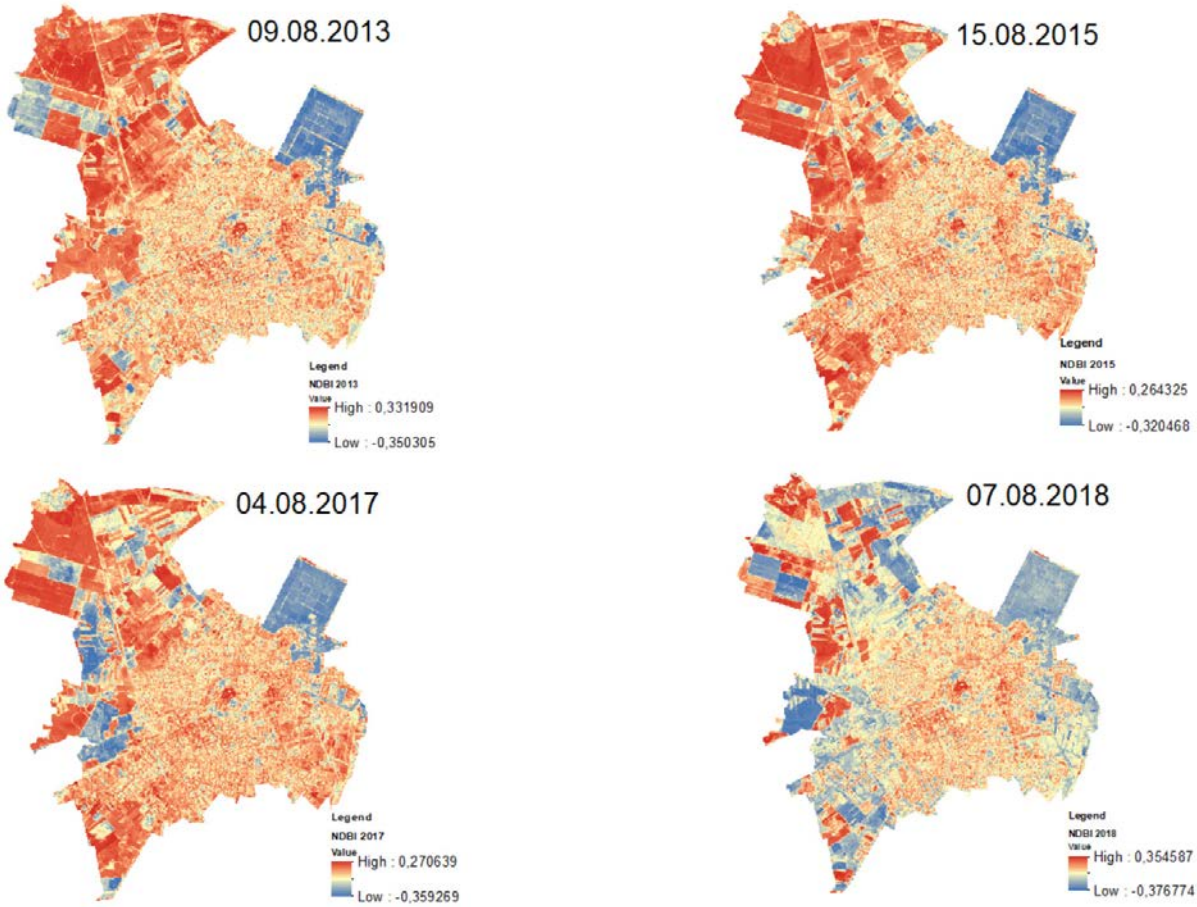

Figure 3. NDBI maps for Timisoara (2013 – 2018)

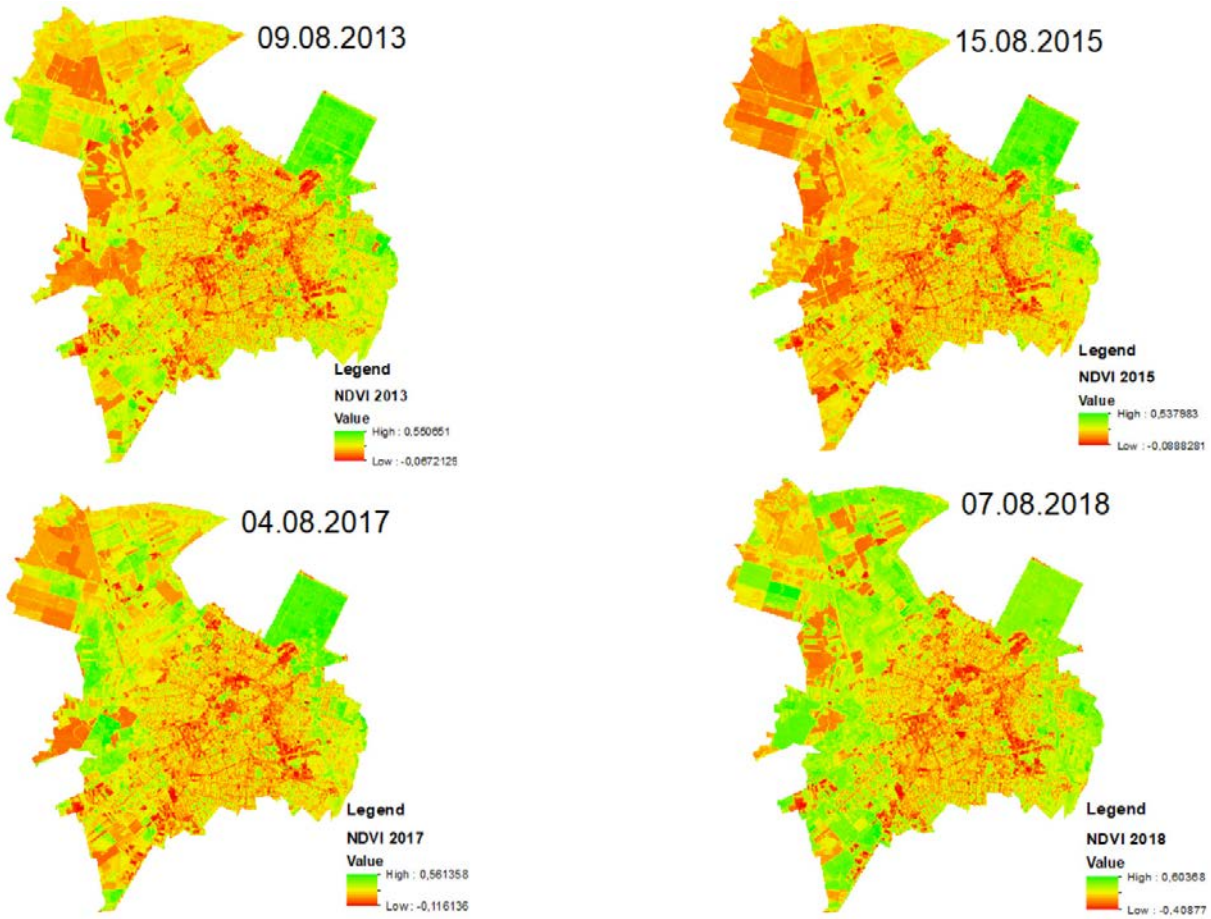

Figure 4. NDVI maps for Timisoara (2013 – 2018)

Weak correlation levels were found for NDVI with TAVG (r = 0.378), for NDVI with PAMT (r =0.553), for LST with PAMT (r =-0.593), and respectively for LST with TAVG (r = -0.655).

These correlation levels found, showed that the values of the two indices (LST and NDVI) are much more strongly influenced by the values of certain months, in the period January - July, than by the average values (ºC) or cumulative (mm) of the climatic parameters. This can indicate in which period waterings would be recommends for the purpose of vegetation management, of course correlated with the climatic conditions, to ensure optimum values of the NDVI index, and indirectly a control of the LST index.

The variation analysis of the indices in relation to the time during the study period, led to the obtaining of polynomial equations that described the behavior of the index's values in statistical accuracy conditions.

The variation of the LST index was most accurately described by a smoothing spline model, under statistical accuracy conditions ($\bar{\varepsilon} = 0.0073$), and the average error was calculated with equation (4). The data from the statistical accuracy parameters of the model are presented in table 2.

$$\bar{\varepsilon} = \left(\sum_{i=1}^{n} \varepsilon_i \right) / n = \left(\sum_{i=1}^{n} \left| \frac{ys_i - y_i}{y_i} \right| \right) / n \quad (4)$$

Table 2. Statistical data related to the spline model

No	x_i	LST			
		y_i	ys_i	ei	$I_{i/1}$
1	0	33.157	33.112	0.0014	1.000
2	736	32.046	32.262	0.0067	0.974
3	1455	33.945	33.528	0.0123	1.013
4	1823	27.988	28.234	0.0088	0.853
				$\bar{\varepsilon} = 0.0073$	

The variation of the NDBI index over the study period was described by a polynomial model of degree 2, equation (5), under conditions of R^2=0.965, p<0.01, F=126.75.

$$NDBI = -6.361E-08x^2 + 8.571E-05x - 0.05641 \quad (5)$$

In the case of the NDVI index, the variation of values with respect to time was described by a polynomial equation of degree 2, equation (6), under conditions of R^2=0.986, p=0.01, F=318.3.

$$NDVI = -7.592E-08x^2 - 0.0001012x + 0.2434 \quad (6)$$

The interdependence relationship between

NDVI and NDBI was described by a linear equation, equation (7), under high statistical accuracy conditions (R^2=0.995, p<0.01, F=2060.01).

$$NDVI = -1.196NDBI + 0.1771 \quad (7)$$

According to this relation, as the value of the NDBI index increases, the value of the NDVI index decreases directly, values highlighted in the spectral information. The values of both indices were present with a variable ratio in the spectral information of the satellite images, associated with the climatic conditions of the study period. In this sense, a very strong negative correlation was found between the two indices (r = -0.998).

It was analyzed how the climatic conditions influenced the variation of the NDVI and LST indices during the study period. Given the level of correlations recorded between NDVI and LST indices with climatic parameters T (ºC) and P (mm), it was analyzed how T and P values influenced the distribution of NDVI and LST.

From the analysis made it was found that the NDVI value for August was determined by the T values for July (T7) and the P values for June (P6), in statistical accuracy condition.

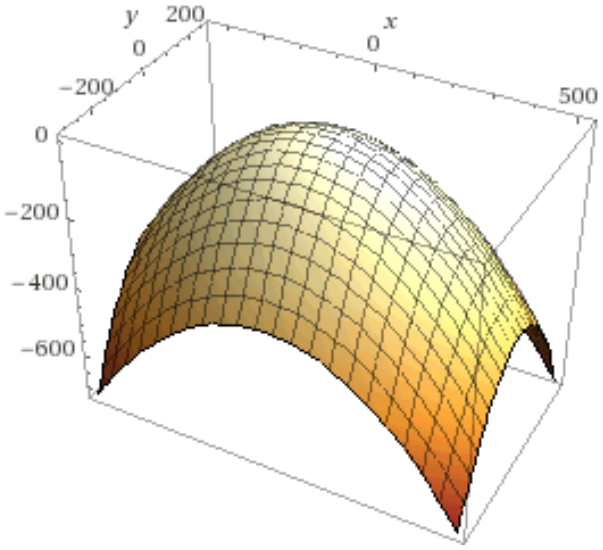

Figure 5. 3D graph for NDVI variation according to T (ºC) in June, and P (mm) in June

Multiple regression analysis led to equation (8) under conditions of R^2=0.998, p<<0.01. A 3D graphical distribution of the NDVI values in relation to T7 (Y7=x) and P6 (P6=y) (Figure 5), was obtained, and a distribution in the form of isoquants which shows the optimal NDVI according to the T7 and P6 values under the study conditions (Figure 6).

$$NDVI = ax^2 + by^2 + cx + dy + exy + f \quad (8)$$

where: x – average temperature (ºC) in July (T7);
y – precipitation (mm) in June (P6);
a, b, c, d, e, f - the equation (8) coefficients*;
a= -0.00164;
b= -0.00415;
c= 0.13119;
d= -0.20018;
e= 0.00384;
f=0.

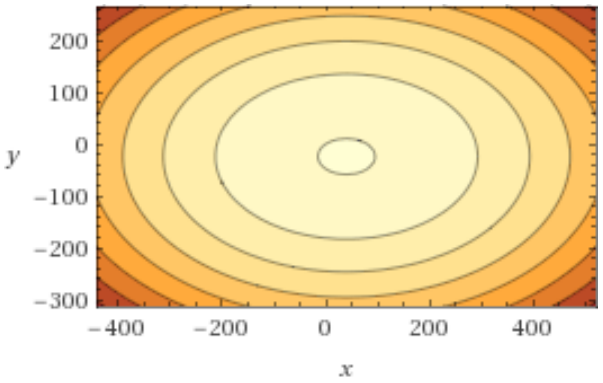

Figure 6. Graphical representation in the form of isoquant for optimal NDVI according to the optimum values of T (ºC) in July and P (mm) in June

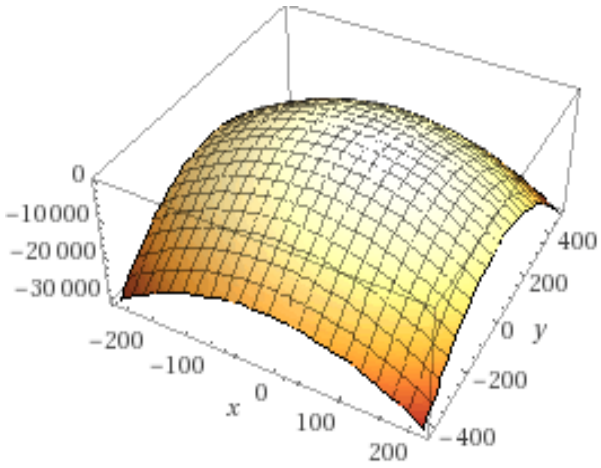

Figure 7. 3D graph for LST variation according to T (ºC) in June, and P (mm) in June

A similar approach was made for the LST index and equation (9) was found that described the variation of the LST index in terms of T7 (average temperature in July, ºC) and P6 (precipitation in June, mm), under conditions of R^2=0.998, p<<0.01. A 3D graphical distribution of LST values in relation to T7 (T7=x) and P6 (P6=y) was obtained (Figure 7).

$$LST = ax^2 + by^2 + cx + dy + exy + f \quad (9)$$

where: x – average temperature (ºC) in July (T7);
y – precipitation (mm) in June (P6);
a, b, c, d, e, f - the equation (9) coefficients**;
a= -0.22844;

b= -0.08851;
c= -9.09043;
d= 6.79466;
e= 0.20676;
f=0.

*, ** - for high accuracy, the values of the coefficients of equations (8) and (9) were 16 decimal digits

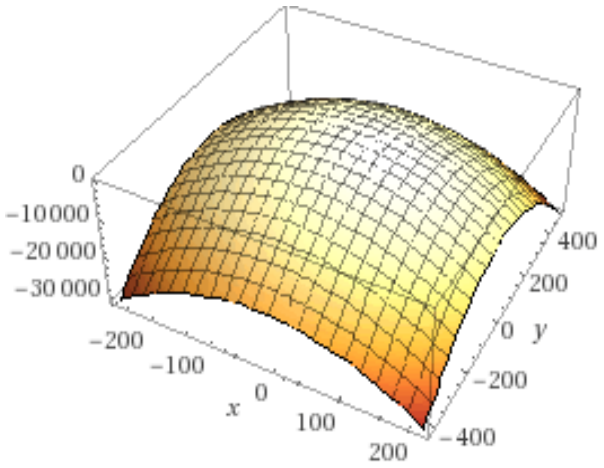

Figure 7. 3D graph for LST variation according to T (ºC) in June, and P (mm) in June

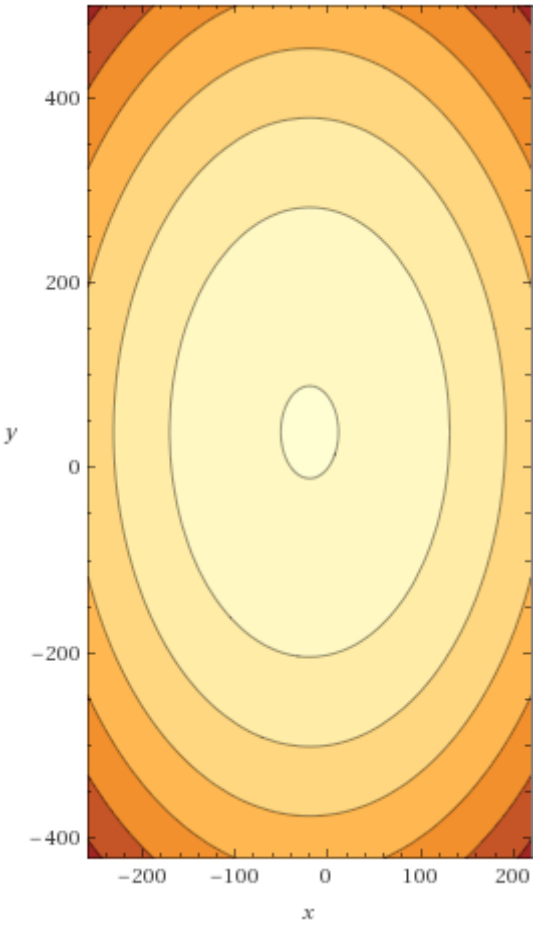

Figure 8. Graphical representation in the form of isoquant for optimal LST according to the optimum values of T (ºC) in July and P (mm) in June

Also, a distribution was obtained in the form of isoquants, which shows the optimum LST according to the thermal values and precipitation in the study conditions (Fig. 8).

4. DISCUSSIONS

The results generated are in accordance with the findings of other studies and research in the use of satellite images and spectral information for the evaluation and characterization of terrestrial areas and in particular urban ones. Spectral information from high resolution images accurately expresses the state and dynamics in time and space of the analyzed surface (Gómez et al., 2016; Khan et al., 2018).

Specific indices calculated based on spectral data facilitated the evaluation of some areas with various geometries and typologies and provided practical solutions for optimization and management (Govedarica et al., 2015; Štrbac et al., 2017; Milanović et al., 2019; Firoozi et al., 2020; Popescu et al., 2020; Sala et al., 2016, 2020).

The NDVI, NDBI and LST indices used in the present study were frequently used and with high efficiency in other studies for the analysis and assessment of urban ecosystems (Bonafoni & Keeratikasikorn, 2018; Guha et al., 2018; Kaplan et al., 2018; Firozjaei et al., 2019; Liu et al., 2019; Wong et al., 2019), and this confirms that the investigation methodology used was well chosen.

Urban areas are highly anthropogenic ecosystems, and imaging technologies have proven useful in the study and management of these ecosystems (Kolcsár & Szilassi, 2018; Świercz & Zajęcka, 2018; Tavares et al., 2019). From the analysis of Landsat images, Zhang et al., (2018) highlighted temporal variation patterns in four cities with strongly anthropized urban ecosystems, in conditions of statistical safety (R^2> 0.80, RMSE <7.2%).

The effect of the heat islands in the urban areas is in strong correlation with the environment built by man and creates discomfort, respectively it affects the human health.

A study conducted in the Toronto City, based on satellite images, reported statistically significant differences between the average thermal values in the area of commercial or industrial land (29.1ºC) compared to the average thermal values in areas with parks or leisure areas (25.1ºC), or areas with water gloss (23.1ºC) (Rinner & Hussain, 2011).

Another study conducted on Skopje City, reported values of the correlation between LST and NDVI of r=-0.63 (2013) and r=-0.59 (year 2017), and between LST and NDBI correlation values of

r=0.67 (2013) and r=0.64 (year 2017) (Kaplan et al., 2018).

Study on Košice locality based on LST (Landsat 8 scenes), in a comparative analysis between urban and rural environment, led to significant differences in condition of $p < 0.001$, and high LST values were associated with industrial urban structures, lack of vegetation and of water surface (Onačillová & Gallay, 2018).

Regarding the variation of LST in relation to NDVI, Onačillová & Gallay (2018) reported for August the correlation value $R2 = 0.693$, and in the present study for August was recorded the correlation value of LST with NDVI at $r = - 0.786$, with a similar statistical significance.

Similar expressions of LST have also been confirmed by other studies in urban areas, such as in the city of Brno (Dobrovolný, 2013), the city of Beijing (Chen et al., 2015), the cities of Florence and Naples (Guha et al., 2018), Raipur city (Guha & Govil, 2020) etc.

The values of the LST index registered very strong and strong correlations with the precipitations of June - July, but also with the temperatures of March, April, and May. The thermal values from March, April and May are important for the beginning of a new vegetation cycle. In this period of the vegetative cycle, the thermal values have a priority role, in the conditions of the water reserve in the soil during the vegetative rest period. Favorable thermal conditions lead to a good start of the vegetation, which will be reflected in the degree of the later vegetal carpet development, so also in the NDVI index values that acurately expresses the vegetation.

Subsequently, with the growth of vegetation and the intensification of the evapotranspiration process, associated with longer and warmer days, the need for water becomes higher for the vegetation in the urban ecosystem. In the conditions of July and August, with the high thermal values specific to this period, but also with the cumulative thermal effect of the radiant surfaces in the city (buildings, roads, parking lots, etc.), the LST index values faithfully reflect the conditions of the urban ecosystem.

The LST / NDVI balance acquires new valences, and in the conditions of a reduced volume of precipitations in the respective period, the waterings are necessary to ensure optimal conditions for the vegetation. A good rainfall regime replaces this water requirement of the plants, but in its absence, maintenance watering is required for all green spaces, even small areas, and these have an important role in urban thermal regulation, a fact confirmed by some studies (Onačillová & Gallay, 2018).

This suggests that water supply of urban green spaces, correlated with precipitation levels, can significantly contribute to ensuring optimal vegetation conditions captured by the NDVI index and to control and manage the appearance of thermal stress, captured at the LST index (Atasoy, 2018; Govil et al., 2019; Wu & Zhang, 2019).

5. CONCLUSIONS

The study of urban areas through satellite images, specific indices and imaging analysis is of interest and also a necessity for assessing the specific environmental conditions of urban ecosystems.

The specific indices LST, NDVI and NDBI were useful tools in the present study to evaluate the temporal variation over a period of five years of the environmental conditions in the city of Timisoara, in close relation with the climatic conditions of temperature and precipitation.

The NDVI index captured the vegetation dynamics in relation to the temperature and precipitation conditions in January - July time interval, for a period of five years (2013 - 2018).

Very strong correlations of NDVI with July precipitation ($r = 0.900$), very strong negative correlations of LST with July precipitation ($r = - 0.976$), very strong negative correlations between NDVI and NDBI ($r = -0.998$) as well as strong positives correlations between LST and NDBI ($r = 0.824$) recommend these indices for the decisions to provide green areas watering, correlated with the volume of precipitation between June and July, and as a model for managing environmental conditions in the city of Timisoara.

It is important even to water the small green surfaces, the urban vegetation contributing to the balance of the NDBI / NDVI / LST relationship and the management of the urban environmental conditions. Watering of radiant heat surfaces (roads, concrete parking lots) can help reduce thermal radiation. Ecological parkings can also contribute to the control of thermal radiation and the reduction of LST values.

The study may be the basis for the development of a model for monitoring and management of the urban ecosystem in the city of Timisoara in order to monitor environmental conditions, especially in the summer season, and water supply interventions for green spaces, reflected in values of NDVI and LST indices, correlated with climatic conditions.

Acknowledgments

The research is supported by the project "Ensuring excellence in the activity of RDI within USAMVBT" code 35PFE, submitted in the competition Program 1 - Development of the national system of research - development, Subprogram 1.2 - Institutional performance, Institutional development projects - Development projects of excellence in RDI.

The authors thanks to the GEOMATICS Research Laboratory, BUASMV "King Michael I of Romania" from Timisoara, for the facility of the software use for this study.

REFERENCES

Anand, M., Gonzalez, A., Guichard, F., Kolasa, J. & Parrott, L., 2010. *Ecological systems as complex systems: challenges for an emerging science*, Diversity, 2, 395-410.

Aram, F., García, E.H., Solgi, E. & Mansournia, S., 2019. *Urban green space cooling effect in cities.* Heliyon, 5, 4, e01339.

Atasoy, M., 2018. *Monitoring the urban green spaces and landscape fragmentation using remote sensing: a case study in Osmaniye, Turkey*. Environmental Monitoring and Assessment 190, 12, 713.

Bianchin, A. & Bravin, L., 2008. *Remote sensing and urban analysis*, In: Gervasi O., Murgante B., Laganà A., Taniar D., Mun Y., Gavrilova M.L. (eds) Computational Science and Its Applications – ICCSA 2008. ICCSA 2008. Lecture Notes in Computer Science, 5072, 300-315.

Bonafoni, S. & Keeratikasikorn, C., 2018. *Land surface temperature and urban density: Multiyear modeling and relationship analysis using MODIS and Landsat data*. Remote Sensing, 10, 1471.

Chen, W., Zhang, Y., Gao, W. & Zhou, D., 2015. *The investigation of urbanization and urban heat island in Beijing based on remote sensing.* Procedia – Social and Behavioral Sciences, 216, 141-150.

Chen, W., Huang, H., Dong, J., Zhang, Y., Tian, Y. & Yang, Z., 2018. *Social functional mapping of urban green space using remote sensing and social sensing data*. ISPRS Journal of Photogrammetry and Remote Sensing, 146, 436-452.

Deng J., Huang Y., Chen B., Tong C., Liu P., Wang H. & Hong Y., 2019. *A methodology to monitor urban expansion and green space change using a time series of Multi-Sensor SPOT and Sentinel-2A images*. Remote Sensing, 11, 1230.

Dobrovolný, P., 2013. *The surface urban heat island in the city of Brno (Czech Republic) derived from land surface temperatures and selected reasons for its spatial variability.* Theoretical and Applied Climatology, 112, 89-98.

Du, P., Liu, P., Xia, J., Feng, L., Liu, S., Tan, K. & Cheng, L., 2014. *Remote sensing image interpretation for urban environment analysis: Methods, system and examples*. Remote Sensing, 6, 9458-9474.

Esri., 2014. *DigitalGlobe, GeoEye, i-cubed*, USDA FSA, USGS, AEX, Getmapping, Aerogrid, IGN, IGP, swisstopo, and the GIS User Community.

Firozjaei, M.K., Sedighi, A., Kiavarz, M., Qureshi, S., Haase, D. & Alavipanah, S.K., 2019. *Automated Built-Up Extraction Index: A new technique for mapping surface Built-Up areas using LANDSAT 8 OLI imagery*. Remote Sensing, 11, 1966.

Firoozi, F., Mahmoudi, P., Amir Jahanshani, S.M., Tavousi, T. & Liu, Y., 2020. *Evaluating various methods of vegetative cover change trend analysis using satellite remote sensing productions (Case study: Sistan Plain in Eastern Iran)*. Carpathian Journal of Earth and Environmental Sciences, 15, 1, 211-222. Doi:10.26471/cjees/2020/015/123.

Gómez, C., White, J.C. & Wulder, M.A., 2016. *Optical remotely sensed time series data for cover classification: A review.* ISPRS Journal of Photogrammetry and Remote Sensing, 116, 55-72.

Govedarica, M., Ristic, A., Herbei, M.V. & Sala, F., 2015. *Object oriented image analysis in remote sensing of forest and vineyard areas*. Bulletin UASVM Horticulture, 72, 2, 362-370.

Govil, H., Guha, S., Dey, A. & Gill, N., 2019. *Seasonal evaluation of downscaled land surface temperature: A case study in a humid tropical city*. Heliyon, 5, 6, e01923.

Guha, S., Govil, H., Dey, A. & Gill, N., 2018. *Analytical study of land surface temperature with NDVI and NDBI using Landsat 8 OLI and TIRS data in Florence and Naples city, Italy*. European Journal of Remote Sensing, 51, 1, 667-678.

Guha, S. & Govil, H., 2020. *An assessment on the relationship between land surface temperature and normalized difference vegetation index.* Environment, Development and Sustainability doi:10.1007/s10668-020-00657-6.

Hammer, Ø., Harper, D.A.T. & Ryan, P.D., 2001, *PAST: Paleontological statistics software package for education and data analysis.* Palaeontologia Electronica, 4, 1, 1-9.

Heymans, A., Breadsell, J., Morrison, G.M., Byrne, J.J. & Eon, C., 2019. *Ecological urban planning and design: a systematic literature review.* Sustainability, 11, 3723.

Ishola, K.A., Okogbue, E.C. & Adeyeri, O.E., 2016. *A quantitative assessment of surface urban heat islands using satellite multitemporal data over Abeokuta, Nigeria.* International Journal of Atmospheric Sciences, 2016, ID3170789.

Kadhim, N., Mourshed, M. & Bray, M., 2016. *Advances in remote sensing applications for urban sustainability*. Euro-Mediterranean Journal for Environmental Integration, 1, 7.

Kaplan, G., Avdan, U. & Avdan, Z.Y., 2018. *Urban heat island analysis using the Landsat 8 satellite data: A case study in Skopje, Macedonia*.

Proceedings, 2, 358.

Khan, M.J., Khan, H.S., Yousaf, A., Khurshid, K. & Abbas, A., 2018. *Modern trends in hyperspectral image analysis: A review*. IEEE Access, 6, 14118-14129.

Kolcsár, R.A. & Szilassi, P., 2018. *Assessing accessibility of urban green spaces based on isochrone maps and street resolution population data through the example of Zalaegerszeg, Hungary*. Carpathian Journal of Earth and Environmental Sciences, 13, 1, 31-36, DOI:10.26471/cjees/2018/013/003.

Kumar, R., Mishra, V., Buzan, J., Kumar, R., Shindell, D. & Huber, M., 2017. *Dominant control of agriculture and irrigation on urban heat island in India*. Scientific Report, 7, 14054.

Lahoti, S., Kefi, M., Lahoti, A. & Saito, O., 2019. *Mapping methodology of public urban green spaces using GIS: An example of Nagpur City, India.* Sustainability, 11, 2166.

Lehoczky, A., Sobrino, J.A., Skokević, D. & Aguilar, E., 2017. *The urban heat island effect in the City of Valencia: A case study for hot summer days.* Urban Science, 1, 1, 9.

Liu, L. & Zhang, Y., 2011. *Urban heat island analysis using the Landsat TM data and ASTER data: A case study in Hong Kong*. Remote Sensing, 3, 7, 1535-1552.

Liu, X., Sherbinin, A.de & Zhan, Y., 2019. *Mapping urban extent at large spatial scales using machine learning methods with VIIRS nighttime light and MODIS daytime NDVI data*. Remote Sensing, 11, 10, 1247.

Matikainen, L. & Karila, K., 2011. *Segment-based land cover mapping of a suburban area - comparison of high-resolution remotely sensed datasets using classification trees and test field points*. Remote Sensing, 3, 8, 1777-1804.

Merschdorf, H., Hodgson, M.E. & Blaschke, T., 2020. *Modeling quality of urban life using a geospatial approach*. Urban Science, 4, 5.

Milanović, M.M., Micić, T., Lukić, T., Nenadović, S.S., Basarin, B., Filipović, D.J., Tomić, M., Samardžić, I., Srdić, Z., Nikolić, G., Ninković, M.M., Sakulski, D. & Ristanović, B., 2019. *Application of landsat-derived NDVI in monitoring and assessment of vegetation cover changes in Central Serbia.* Carpathian Journal of Earth and Environmental Sciences, 14, 1, 119-129, DOI:10.26471/cjees/2019/014/064.

Moskal, M., Styers, D.M. & Halabisky, M., 2011. *Monitoring urban tree cover using object-based image analysis and public domain remotely sensed data*. Remote Sensing, 3, 10, 2243-2262.

Nielsen, M.M., 2015. *Remote sensing for urban planning and management: The use of window-independent context segmentation to extract urban features in Stockholm*. Computers, Environment and Urban Systems, 52, 1-9.

Označillová, K. & Gallay, M., 2018. *Spatio-temporal analysis of surface urban heat island based on Landsat ETM+ and OLI/TIRS imagery in the City of Košice, Slovakia*. Carpathian Journal of Earth and Environmental Sciences, 13, 2, 395-408, DOI:10.26471/cjees/2018/013/034.

Oncia, S., Herbei, M. & Popescu, C., 2013a. *Study of territorial and infrastructure development in the Petrosani city - The Hunedoara County using GIS elements*. Journal of Environmental Protection and Ecology, 14, 1, 225-232.

Oncia, S., Herbei, M. & Popescu, C., 2013b. *Sustainable development of the Petrosani City, the Hunedoara County based on GIS analysis*. Journal of Environmental Protection and Ecology, 14, 3, 232-240.

Orusa, T. & Mondino, E.B., 2019. *Landsat 8 thermal data to support urban management and planning in the climate change area: a case study in Torino area, NW Italy*. Proc. SPIE 11157, Remote Sensing Technologies and Applications in Urban Environments IV, 111570O.

Planet Team, 2018. *Planet application program interface*: In Space for Life on Earth; Planet Team: San Francisco, CA, USA, 2018. Available online: https://api.planet.com

Popescu, C.A., Herbei, M.V. & Sala, F., 2020. *Remote sensing in the analysis and characterization of spatial variability of the territory*. Scientific Papers Series Management, Economic Engineering in Agriculture and Rural Development, 20, 1, 505-514.

Pickett, S.T.A., Cadenasso, M.L., Childers, D.L., McDonnell, M.J. & Zhou, W., 2016. *Evolution and future of urban ecological science: ecology in, of, and for the city*. Ecosystem Health and Sustainability, 2, 7, e01229.

Qin, K., Rao, L., Xu, J., Bai, Y., Zou, J., Hao, N., Li, S. & Yu, C., 2017. *Estimating ground level NO_2 concentrations over Central-Eastern China using a satellite-based geographically and temporally weighted regression model*. Remote Sensing, 9, 950.

Rakhshandehroo, M., Yusof, M.J.M., Arabi, R. & Jahandarfard, R., 2016. *Strategies to improve sustainability in urban landscape*. Journal of Landscape Ecology, 9, 3, 5-13.

Rasul, A., Balzter, H. & Smith, C., 2015. *Spatial variation of the daytime Surface Urban Cool Island during the dry season in Erbil, Iraqi Kurdistan, from Landsat 8*. Urban Climate, 14, 2, 176-186.

Rinner, C. & Hussain, M., 2011. *Toronto's Urban Heat Island - exploring the relationship between land use and surface temperature*. Remote Sensing, 3, 6, 1251-1265.

Rouse, J.W.Jr., Haas, R.H., Schell, J.A. & Deering, D.W., 1974. *Monitoring vegetation systems in the Great Plains with ERTS.* Third Earth Resource Technology Sattelite - 1 Symposium, NASA SP-351(I), 309-317.

Sala, F., Rujescu, C. & Constantinescu, C., 2016, *Causes and solutions for the remediation of the poor allocation of P and K to wheat crops in Romania*. AgroLife Scientific Journal, 5, 1, 184-193.

Sala, F., Popescu, C.A., Herbei, M.V. & Rujescu, C., 2020. *Model of color parameters variation and correction in relation to "Time-View" image acquisition effects in wheat crop*. Sustainability, 12, 6, 2470.

SMT-Statia Meteorologica Timisoara, 2019. *Date climatice (Timisoara Meteorological Station - Climate data)*, 2013 - 2018.

Štrbac, O., Milanović, M. & Ogrizović, V., 2017. *Estimation the evapotranspiration of urban parks with field based and remotely sensed datasets.* Carpathian Journal of Earth and Environmental Sciences, 12, 2, 605-616.

Świercz, A. & Zajęcka, E., 2018. *Accumulation of heavy metals in the urban soils of the city of Skarżysko-Kamienna (Poland) with regard to land use*. Carpathian Journal of Earth and Environmental Sciences, 13, 1, 249-266, DOI:10.26471/cjees/2018/013/022

Tarantino, E. & Figorito, B., 2011. *Extracting buildings from true color stereo aerial images using a decision making strategy*. Remote Sensing, 3, 8, 1553-1567.

Tavares, P.A., Beltrão, N., Giomarães, U.S., Teodoro, A. & Golçalves, P., 2019. *Urban ecosystem services quantification through remote sensing approach: A systematic review*. Environments, 6, 51.

Tran, T.D.-B., Puissant, A., Badariotti, D. & Weber, C., 2011. *Optimizing spatial resolution of imagery for urban form detection - The cases of France and Vietnam*. Remote Sensing, 3, 10, 2128-2147.

Wan, B., Guo, Q., Fang, F., Su, Y. & Wang, R., 2015. *Mapping US urban extents from MODIS data using One-Class classification method*. Remote Sensing, 7, 8, 10143-10163.

Van, T.T., Tran, N.D.H., Bao, H.D.X., Phuong, D.T.T., Hoa, P.K. & Han, T.T.N., 2017. *Optical remote sensing method for detecting urban green space as indicator serving city sustainable development*. Proceedings, 2, 140.

Weng, Q., Lu, D. & Schubring, J., 2004. *Estimation of land surface temperature–vegetation abundance relationship for urban heat island studies*. Remote Sensing of Environment, 89, 467-483.

Weng, Q., Firozjaei, M.K., Sedighi, A., Kiavarz, M. & Alavipanah, S.K., 2018. *Statistical analysis of surface urban heat island intensity variations: A case study of Babol city, Iran.* GIScience & Remote Sensing, 56, 4, 576-604.

Wolfram, Research, Inc., Mathematica, Version 12.1, Champaign, IL (2020).

Wong, M.M.F., Fung, J.C.H. & Yeung, P.P.S., 2019. *High-resolution calculation of the urban vegetation fraction in the Pearl River Delta from the Sentinel-2 NDVI for urban climate model parameterization*, Geoscience Letters, 6, 2.

Wu, Z. & Zhang, Y., 2019. *Water bodies' cooling effects on urban land daytime surface temperature: Ecosystem service reducing heat island effect*. Sustainability, 11, 787.

Yuchechen, A., Lakkis, S.G. & Canziani, P., 2017. *Linear and non-linear trends for seasonal NO_2 and SO_2 concentrations in the Southern Hemisphere (2004–2016)*. Remote Sensing, 9, 891.

Zha, Y., Gao, Y. & Ni, S., 2003. *Use of normalized difference built-up index in automatically mapping urban areas from TM imagery*. International Journal of Remote Sensing, 24, 583-594.

Zhang, H., Wang, T., Zhang, Y., Dai, Y., Jia, J., Yu, C., Li, G., Lin, Y. & Cao, Y., 2018. *Quantifying short-term urban land cover change with time series Landsat data: A comparison of four different cities.* Sensors, 18, 4319.

Zhou, D., Xiao, J., Bonafoni, S., Berger, C., Deilami, K., Zhou, Y., Frolking, S., Yao, R., Qiao, Z. & Sobrino, J.A., 2018. *Satellite remote sensing of surface urban heat islands: Progress, challenges, and perspectives*. Remote Sensing, 11, 48.

Zobec, M., Betz, O. & Unterweger, P.A., 2020. *Perception of urban green areas associated with sociodemographic affiliation, structural elements, and acceptance stripes*. Urban Science, 4, 9.

Received at: 06. 04. 2020
Revised at: 29. 05. 2020
Accepted for publication at: 10. 06. 2020
Published online at: 19. 06. 2020